

# A Sensing Chair Using Pressure Distribution Sensors

Hong Z. Tan, *Member, IEEE*, Lynne A. Slivovsky, *Student Member, IEEE*, and Alex Pentland, *Member, IEEE*

**Abstract**—One challenge in multimodal interface research is the lack of robust subsystems that support multimodal interactions. By focusing on a chair—an object that is involved in virtually all human–computer interactions, the sensing chair project enables an ordinary office chair to become aware of its occupant’s actions and needs. Surface-mounted pressure distribution sensors are placed over the seatpan and backrest of the chair for real time capturing of contact information between the chair and its occupant. Given the similarity between a pressure distribution map and a grayscale image, pattern recognition techniques commonly used in computer and robot vision, such as principal components analysis, have been successfully applied to solving the problem of sitting posture classification. The current static posture classification system operates in real time with an overall classification accuracy of 96% and 79% for familiar (people it had *felt* before) and unfamiliar users, respectively. Future work is aimed at a dynamic posture tracking system that continuously tracks not only steady-state (static) but transitional (dynamic) sitting postures. Results reported here form important stepping stones toward an intelligent chair that can find applications in many areas including multimodal interfaces, intelligent environment, and safety of automobile operations.

**Index Terms**—Haptic sensing, posture classification, posture-based interface, pressure-distribution sensors, sensing chair.

## I. INTRODUCTION

AS COMPUTING becomes more ubiquitous and distributed, there is a growing need for human–computer interfaces that support a new interaction paradigm. Efforts are currently underway to develop a novel haptic interface system around an object that is involved in virtually all human–computer interactions, yet has so far remained sensory and information deprived—a chair. The chair is said to be sensory deprived because it can not sense the actions of its occupant and therefore can not interpret the user’s intentions. The chair is said to be information deprived because it does not provide any useful information to its occupant. The chair that is available today is, therefore, a passive object that does not respond to its user’s needs.

To enable a chair to sense and interpret its occupant’s actions, pressure distribution sensors are surface-mounted on the seatpan and backrest of a *sensing chair*. To enable a chair to de-

liver useful information to its occupant, vibrotactile stimulators are embedded in a *chair display* [27], [28]. This paper reports our work on the sensing chair. Our work is motivated by the desire to transform ordinary chairs into *perceptual* and *multimodal* human–computer interfaces.

### A. Why Perceptual User Interfaces?

Because a computer can not act intelligently or be helpful if it is not aware of its user [20]. Today’s computers are blind, deaf, and deafferented (except for their awareness of keystrokes and mouse clicks). Tomorrow’s computers will be able to see, hear, and touch the environment, as well as people who interact with them. Only then can a computer become situation aware and helpful—like an invisible butler [20]. Numerous systems have been developed that explore the idea of perceptual intelligence where computers are equipped with sensory mechanisms similar to our own (for example, vision through cameras, and hearing through microphones) [4], [8], [9], [15], [22], [29]–[31]. Among those, very few employ touch-based sensory information. The sensing chair project is conceptualized to explore the use of *distributed* pressure information, from sensors that are analogous to artificial skin, to achieve perceptual intelligence.

Perceptual intelligence for a computer can not be achieved by merely collecting and displaying sensory information, like what most webcams do. Perceptual intelligence results from an *understanding* of what the sensory data reveal about the *state* of the environment and people. The key research problem to be addressed with the sensing chair, therefore, is the automatic processing and interpretation of touch sensor information, and the modeling of user behavior leading to such sensory data. We envision tomorrow’s computing environment where all objects are outfitted with a layer of artificial skin (for example, a sensing chair, a sensing floor, a sensing file folder). We expect the algorithms and behavior models that we develop with the sensing chair to be extensible to large-scale distributed haptic sensing and interpretation.

### B. Why Multimodal Interfaces?

Because humans naturally employ multimodal information channels for communication, and because multimodal interfaces have been demonstrated to be effective [19]. Cognitive research has shown that multimodal communication results in increased amount of transmitted information [14]. It has been shown that a signal with a single varying attribute can at most transmit 2–3 bits to a human observer (for example, we can only identify about 5–7 loudness levels of a fixed-frequency pure tone). However, greater information transmission can be achieved by employing signals with multiple attributes (for example, one can easily identify hundreds of faces at a glance of a person or a photograph, because many facial

Manuscript received March 28, 2000; revised February 20, 2001. Recommended by Guest Editor N. Xi. This work was supported in part by British Telecom, Things That Think consortium at the M.I.T. Media Laboratory, Steelcase NA, a Research Grant from Purdue Research Foundation, and by a National Science Foundation Faculty Early Career Development (CAREER) Award under Grant 9984991-IIS.

H. Z. Tan and L. A. Slivovsky are with the Haptic Interface Research Laboratory, Purdue University, West Lafayette, IN 47907 USA (e-mail: hongtan@purdue.edu; lynnes@purdue.edu).

A. Pentland is with the Media Laboratory, Massachusetts Institute of Technology, Cambridge, MA 02139 USA (e-mail: sandy@media.mit.edu).

Publisher Item Identifier S 1083-4435(01)08147-9.

features contribute to the overall appearance of a face). This increase in transmitted information can be obtained whether multiple modalities convey different information or encode the same information redundantly [14]. Therefore, multimodal interfaces facilitate more natural and efficient human-computer interactions.

One challenge in multimodal interface research is the lack of multimodal interface systems. Robust systems for applications such as speech recognition or gesture interpretation require long-term research and development efforts from a multidisciplinary team of investigators. True multimodal interactions can not take place until problems in each of these application domains are solved. Our work focuses on the development of a single-modality (haptic) interface system that can be integrated with other state-of-the-art interface systems to enable the next generation of computer users to interact naturally with computers.

Our long-term goal with the sensing chair project is to develop a chair-based haptic sensing system that is robust enough to drive many real-time applications. In the case of an intelligent environment, for example, a sensing chair can allow a seated participant to use sitting postures to directly control a video camera in the remote conference room. Imagine zooming in on the remote speaker by leaning forward, or panning the remote camera by rotating the chair! With regard to ergonomics, a sensing office chair can gather the information needed by a "virtual posture coach" to help a computer user maintain proper sitting postures. This can be especially helpful when long-term monitoring is required due to previous ailments such as neck or back injuries. Our sensing chair system can also help furniture designers evaluate their new chairs by observing how people sit in the chairs over an extended period of time. In the area of rehabilitation, a sensing wheelchair can monitor the pressure buildup in the chair, and trigger mechanisms such as surface air bladders to redistribute pressure distribution on the chair surface. A system like this can be especially beneficial to individuals with impaired mobility. Finally, a sensing driver's or passenger's seat can automatically adjust an airbag's deployment force according to the estimated weight and size of the driver, or disable the airbag if an infant car seat is detected in the front seat.

## II. RELATED WORK

In the interest of space and due to a body of literature that is scattered in many disciplines, a full review is not presented here. Instead, we contrast our sensing chair with projects on chair-based systems and on the use of pressure distribution sensors.

### A. Chair-Based Systems

Many systems have been developed around the structure of a chair. The British Telecom SmartSpace, for example, is a concept personal working environment of the future, built around a swivel chair.<sup>1</sup> It is equipped with a horizontal LCD touchscreen, video projection, and 3-D sound space. In contrast, the goal of our sensing chair is to achieve information extraction and display by instrumenting the chair itself.

<sup>1</sup><http://www.bt.com/innovation/exhibition/smartspace/index.htm>.

BCAM International (Melville, NY) has developed a recliner with pneumatically controlled air bladders placed near the surface of the recliner that can be inflated to "hug" and support the body.<sup>2</sup> This technology, called the "intelligent surface," has recently been implemented in the United Airline's connoisseur class seats [7], [24]. It should be pointed out that the air bladder activation patterns are based on ergonomic considerations, rather than on the needs of its occupant. The sensing chair can provide the needed intelligence to such mechanisms so that surface distribution can be altered *in response to* the real-time pressure distributions in the chair in an ergonomically beneficial manner.

### B. Pressure Sensing

Pressure distribution sensors have been widely used for the evaluation of weight supporting surfaces in shoes, chairs, and beds. Examples of shoe studies include the assessment of seven types of shoes with regard to their ability to reduce peak pressure during walking for leprosy patients [2], the evaluation of the generalizability of in-shoe peak pressure measures with data collected from numerous subjects over a period of time using two calibration schemes [16], and the validation of the use of total contact casts for healing plantar neuropathic ulcerations through reduction of pressure over the ulcer [6]. Studies of seats include the development of a measurement protocol and analysis technique for assessing pressure distribution in office chairs [23], the use of body pressure distribution measures as part of a series of tests for assessing comfort associated with five automobile seats [12], and an interesting review of how objective pressure measures can lead to improved aircrew seating with more evenly distributed pressure patterns, thereby potentially improving a pilot's task performance by reducing or eliminating pain endured during high-acceleration maneuvers of the aircraft [5]. Examples of bed studies include an investigation of support surface pressure and reactive hyperemia (the physiological response to pressure) in older population [1], and a recent development of body posture estimation system for sleepers based on pressure distribution measures and a human skeletal model [11]. Our sensing chair project is similar to the last study cited [11] in that we focus on the automatic processing and interpretation of contact sensor information, whereas the other studies rely on expert analysis of pressure distribution measures. Of particular importance is the development of real-time systems that can be used to drive other processes such as the automatic control of airbag deployment force based on the size, weight, and sitting posture of a driver or passenger.

## III. THE SENSING CHAIR SYSTEM

### A. Overview

To begin with, we are interested in modeling the sitting postures of the person occupying the sensing chair (Fig. 1). As shown in Fig. 2, the sensing chair project is further divided into the two components of static posture classification (identification of steady-state sitting postures), and dynamic posture tracking (continuous tracking of steady state, as well as transi-

<sup>2</sup>The first author was given a demo of a prototype at BCAM International.



Fig. 1. The sensing chair.

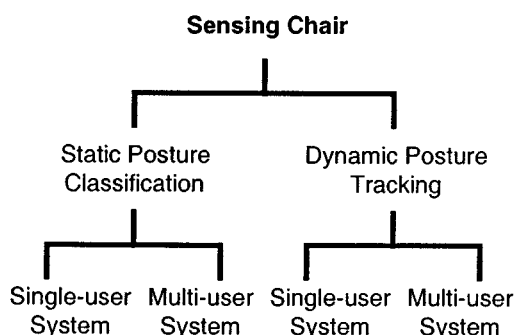


Fig. 2. Overview of the sensing chair project.

tional sitting postures). In each case, we start with a single-user system and proceed to a multiuser system. Our goal is a robust, real-time, and user-independent<sup>3</sup> sitting posture tracking system.

This paper presents our approach and results on a static posture classification system. Given the similarity between a pressure map and an 8-b grayscale image (see Fig. 3), it is speculated that pattern recognition algorithms developed for computer vision would be applicable to the interpretation of sitting postures from pressure distribution data. There are two major approaches to object representation and recognition in computer vision: model-based (for example, [3]) and appearance-based (for example, [17]). The latter is considered more applicable since the concept of object model does not apply directly to pressure maps. Our work is based primarily on the technique of principal components analysis (PCA), also known as “eigenspace methods,” “eigendecomposition,” or “Karhunen–Loeve expansion” [10]. It has been successfully applied to the problem of computer face recognition (e.g., [21], [32]). Our algorithm is presented in Section IV.

<sup>3</sup>By user independence, we refer to a system that works for people who have not contributed to a training database, but whose anthropometry is well represented by the database.

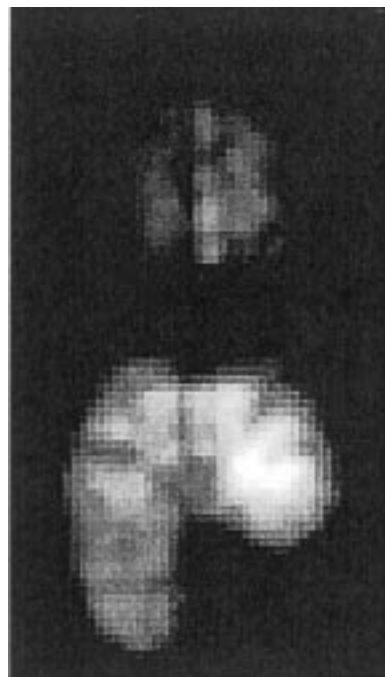


Fig. 3. A full pressure map for the posture “left leg crossed” shown as a 2-D grayscale image. The top, bottom, left, and right sides of the map correspond to the shoulder area, knee area, right side, and left side of the occupant, respectively.

#### B. Hardware Configuration and Preprocessing of Pressure Data

Our sensing chair is equipped with a commercially available pressure distribution sensor called the body pressure measurement system (BPMS) manufactured by Tekscan, Inc. (South Boston, MA). The office chair shown in Fig. 1 is fitted with two sensor sheets (hidden inside the protective pouches) on the seatpan and the backrest. The BPMS system has been selected for: 1) its high resolution (10-mm interelement distance); 2) the flexibility of the sensor sheets (0.10 mm in thickness) so they can conform to the shape of a chair; 3) its usage by major research and industry laboratories including Natick Army Research Lab (for design of army boots) and Steelcase NA and Herman Miller (for chair evaluation); and 4) most importantly, Tekscan’s willingness to provide an API that made it possible for us to access and manipulate pressure distribution data in real time. Each sensor sheet has an array of 42-by-48 pressure sensing elements. Each sensing element outputs an 8-bit digital value proportional to the local pressure. Although the sensor sheets can be calibrated to display pressure readings in PSI or other standard units, the raw digital data are used since we are only interested in the *relative* pressure distribution patterns on the chair surfaces.

The image in Fig. 3 is a full pressure map for the static sitting posture of left leg crossed (after noise removal), shown as a 2-D grayscale image. The top and bottom halves of the pressure map correspond to the pressure distribution on the backrest and seatpan, respectively. To understand the orientation of the pressure map, imagine standing in front of the chair and its occupant, and unfolding the chair so that the backrest and the seatpan lie in

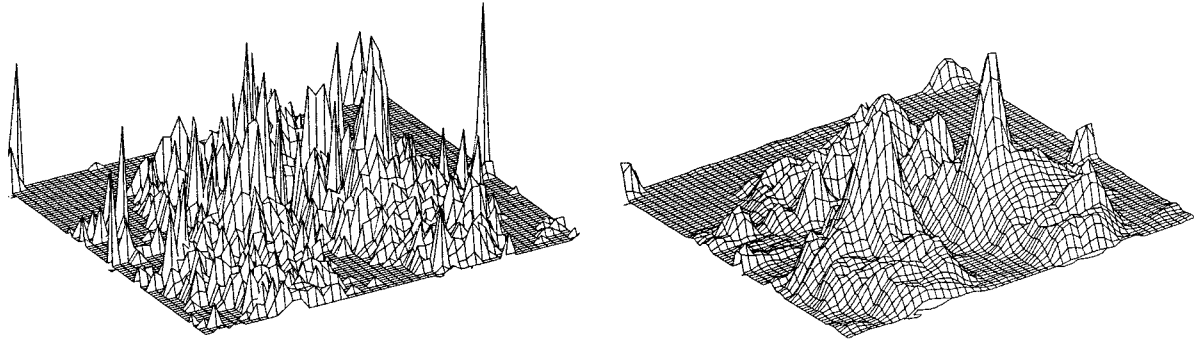


Fig. 4. 3-D views of a pressure map for the posture "seated upright," before (left) and after (right) smoothing.

the same plane. Therefore, the top, bottom, left and right sides of the pressure map shown in Fig. 3 correspond to the shoulder area, knee area, right, and left sides of the occupant, respectively. The size of each full pressure map is 84-by-48 ( $2 \times 42$ -by-48), or 4,032 pixels.

The raw pressure distribution map is typically noisy (spikes in the left image of Fig. 4). The noise is removed by convolving the pressure map with a 3-by-3 smoothing kernel

$$\frac{1}{7} \begin{bmatrix} 0.5 & 1 & 0.5 \\ 1 & 1 & 1 \\ 0.5 & 1 & 0.5 \end{bmatrix}.$$

The smoothed pressure map (right image of Fig. 4) contains pressure artifacts (at the top left and right corners of the image) due to the corners of pressure sensor sheets being wrapped around the chair. Since these artifacts are common to all pressure maps, their removal is not necessary. Finally, the values of pressure readings are normalized, separately for the seatpan and the backrest maps. The rest of this paper assumes that all pressure maps have gone through the aforementioned preprocessing procedures.

#### IV. STATIC POSTURE CLASSIFICATION

##### A. Overview of PCA-Based Classification Algorithm

The key to a PCA-based approach is to reduce the dimensionality of data representation by finding the principal components of the distribution of pressure maps, or equivalently, the eigenvectors of the covariance matrix of a set of training pressure maps. Our PCA-based static posture classification algorithm involves two separate steps: training and posture classification. In the first step, training data for a set of  $K$  predefined static postures are collected. Pressure maps corresponding to the same posture are used to calculate the eigenvectors that best represent the variations among them. This eigenspace, termed *eigenposture space* in this paper, is analogous to the *view-based or modular eigenspace* for face recognition in [21]. Fig. 5 illustrates the process of computing one such eigenposture space. Each of a total of  $M$  training pressure maps is raster-scanned to form a vector of 4032 elements ( $P_m$ ,  $m = 1, \dots, M$ ). These vectors are first de-meanned where  $\bar{P}$  is the average of the  $M$  vectors. The mean-adjusted vectors,  $\Phi_m$  ( $m = 1, \dots, M$ ), are then used to compute the covariance matrix  $\mathbf{C}$ , from which a

##### Calculation of One Eigenposture Space

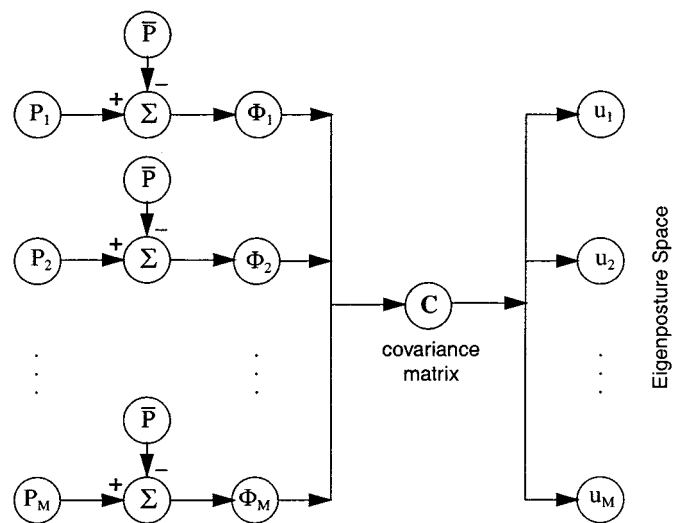


Fig. 5. A diagram for eigenposture space calculation.

set of  $M$  eigenvectors ( $u_i$ ,  $i = 1, \dots, M$ ) are calculated<sup>4</sup> such that their corresponding eigenvalues ( $\lambda_i$ ,  $i = 1, \dots, M$ ) are monotonically decreasing ( $\lambda_1 \geq \lambda_2 \dots \geq \lambda_M$ ). These eigenvectors ( $u_i$ ) can be thought of as forming an  $M$ -dimensional eigenposture space where a 4032-element pressure map can be represented by the  $M$  weights of its projection onto this eigenspace. We have thus effectively reduced the representation of each pressure map from a 4032-dimensional space to an  $M$ -dimensional space. Furthermore, we can choose to use only the first  $M'$  ( $M' < M$ ) eigenvectors whose eigenvalues are the largest to further improve computational efficiency (see Section V). The process shown in Fig. 5 is repeated for all static postures. Note that the calculation of eigenposture spaces is performed off line.

Given a test pressure map  $P_t$ , the second step of posture classification proceeds as follows in real time (Fig. 6). The test map ( $P_t$ ) is first projected onto the eigenposture spaces calculated during the training step. This is done by subtracting the average

<sup>4</sup>It is computationally more feasible to first compute the eigenvectors of  $\mathbf{C}^T$ , and then convert them to the corresponding eigenvectors of  $\mathbf{C}$  (see [32] for details). Alternatively, the method of singular value decomposition (SVD) can be used, recognizing the fact that the eigenvectors of  $\mathbf{C}$  are the left singular vectors of the training data matrix  $X = [\Phi_1 \Phi_2 \dots \Phi_M]$  [see [18] for details].

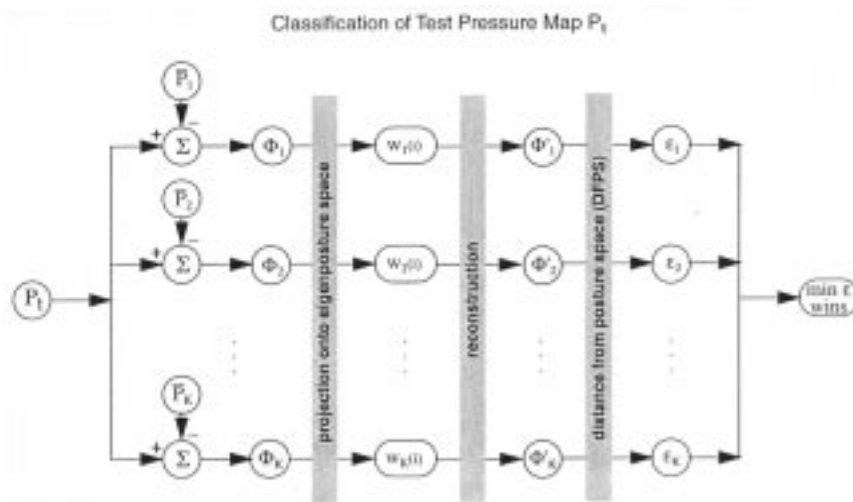


Fig. 6. A diagram for pressure map classification.

pressure map ( $\bar{P}_k$ ,  $k = 1, \dots, K$ ) for each posture from  $P_t$ , and finding the inner dot product of the mean-adjusted posture map ( $\Phi_k$ ,  $k = 1, \dots, K$ ) with each of the eigenvectors in the corresponding eigenposture space. The result is a point in  $k$ th eigenposture space specified by the weights  $w_k(i) = \Phi_k^T \cdot u_i$ , where  $u_i$  denotes the  $i$ th eigenvector in the  $k$ th eigenposture space. These weights are used to calculate the reconstruction of  $P_t$  in each of the eigenposture spaces as  $\Phi'_k = \sum w_k(i) \cdot u_i$ . The distances between  $P_t$  and its  $K$  reconstructions, the so-called distance from posture space (DFPS), can then be computed as  $\varepsilon_k^2 = \|\Phi_k - \Phi'_k\|^2$ . To the extent that  $P_t$  is well represented by one of the  $K$  eigenposture spaces (as indicated by a minimum  $\varepsilon_k$ ), the corresponding posture label ( $k$ ) is used to classify  $P_t$ .

### B. A Single-User Static Posture Classification System

As a proof of concept, a single-user static posture classification system was implemented on a Pentium PC in Windows 3.11 environment (required by the hardware driver) [26], [27]. Training data on a total of  $K = 14$  sitting postures, and  $M = 10$  pressure distribution samples per posture were collected on the first author. The postures were: 1) seated upright; 2) leaning forward; 3) leaning left; 4) leaning right; 5) right leg crossed (with knees touching); 6) right leg crossed (with right foot on left knee); 7) left leg crossed (with knees touching); 8) left leg crossed (with left foot on right knee); 9) left foot on seatpan under right thigh; 10) right foot on seatpan under left thigh; 11) leaning left with right leg crossed; 12) leaning right with left leg crossed; 13) leaning back; and 14) slouching. These postures were considered to be representative of the typical sitting postures that can be found in an office environment [13]. During the training step,  $K = 14$  eigenposture spaces were calculated, each from  $M = 10$  pressure distribution samples. During classification, a new pressure distribution map was first tested for “empty seat” by comparing the sum of all pixel values with a preset threshold. Once a pressure map passed this initial test, it was projected onto the 14 eigenposture spaces and the smallest DFPS,  $\varepsilon_{\min}$ , was found. If  $\varepsilon_{\min}$  was below a preset threshold value, then the corresponding eigenposture space was used to

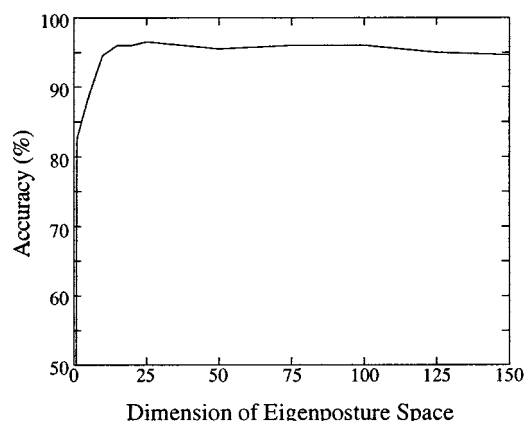


Fig. 7. Classification accuracy for “familiar” subjects.

label the new pressure map. Otherwise, the system declared the posture to be “unknown.”

This single-user system was able to classify sitting postures of the first author with an average accuracy of over 95%. Encouraged by this result, but realizing that the system had to be retrained for each new user, we quickly moved to a multiuser static posture classification system.

### C. A Multiuser Static Posture Classification System

Our current multiuser static posture classification system has been implemented on a Pentium PC in Windows 98 environment [25]. In order to facilitate the training and evaluation of this system, a static posture database has been collected on 30 subjects (15 females and 15 males) for  $K = 10$  sitting postures. The subjects are selected with the goal to cover a wide distribution of anthropometric measurements. The ranges of subject’s height, weight, and age are 152–191 cm, 45.5–118.2 kg, and 18–60 years old, respectively. Each subject has contributed five pressure distribution samples per posture. There are therefore  $M = 150$  training samples per posture, and the training database consists of a total of 1500 pressure distribution maps.<sup>5</sup>

<sup>5</sup>Our static posture database is available [online] at [http://www.ece.purdue.edu/HIRL/projects\\_chair.html](http://www.ece.purdue.edu/HIRL/projects_chair.html).

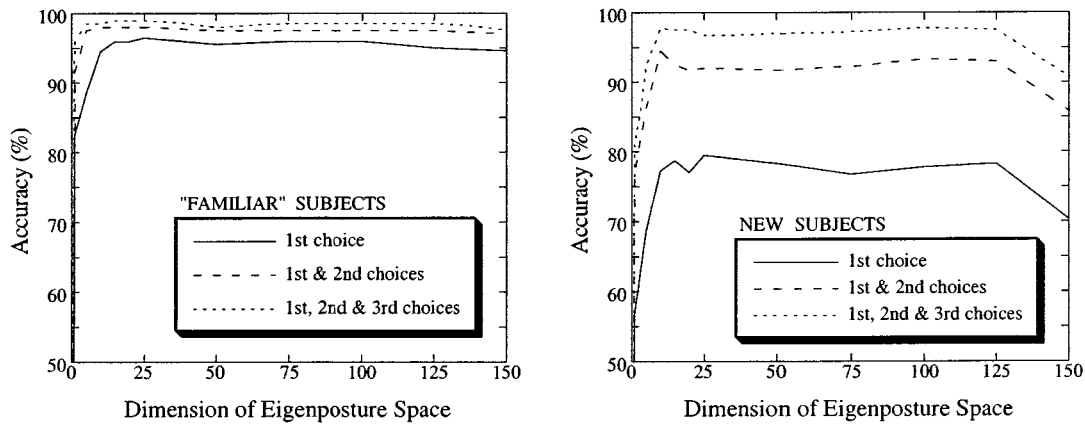


Fig. 8. Classification accuracy for “familiar” and new subjects. Solid, dashed and dotted lines correspond to accuracies associated with the smallest  $\varepsilon$  value, first two smallest  $\varepsilon$  values, and the first three smallest  $\varepsilon$  values, respectively.

The postures contained in the Static Posture Database are: i) seated upright; ii) leaning forward; iii) leaning left; iv) leaning right; v) right leg crossed; vi) left leg crossed; vii) leaning left with right leg crossed; viii) leaning right with left leg crossed; ix) leaning back; and x) slouching. These postures are similar to the 14 postures utilized in the single-user system with two exceptions. First, the two types of leg crossing (one with knees touching, the other with a foot on the other knee) have been combined, thus postures 5) and 6) are now v), and postures 7) and 8) are now vi). Second, the two postures that require a subject to sit on a foot, namely 9) and 10), have been eliminated because some subjects are unable to do so.

The training of a multiuser static posture classification system is essentially the same as that of a single-user system, except that the  $M = 150$  pressure maps used to calculate each eigenposture space (Fig. 5) contain samples from 30 subjects instead of one. The classification step is identical for the single- and multiuser systems. With the implementation of this multiuser static posture classification system, it is now possible to systematically evaluate its performance, and to investigate issues such as the user-independence of such a system.

## V. PERFORMANCE EVALUATION

Accuracy of our static posture classification system has been evaluated with additional pressure maps collected from two groups of subjects. First, an additional 200 pressure distribution maps have been collected from 20 of the 30 subjects who contributed to the static posture database (one sample per posture per subject). These pressure maps are then labeled with respect to their corresponding postures by the static posture classification system. Fig. 7 shows the classification accuracy in terms of percent-correct scores averaged over postures, as a function of the number of eigenvectors ( $M'$ ) that are used in the classification algorithm. As expected, overall classification accuracy increases as a function of the dimension of eigenposture space  $M'$ . The curve shown in Fig. 7 has a knee point at  $M' = 15$  with a corresponding average accuracy of 96%.

Classification accuracy by posture (averaged across subjects) ranges from 90.3% (for posture “leaning back”) to 99.8% (for “slouching”). The system is also able to discern among pos-

tures that have very similar pressure distribution maps (for example, 95.2% for “leaning left,” 95.1% for “right leg crossed,” and 93.5% for “leaning left with right leg crossed”).

Secondly, a total of 400 pressure distribution maps have been collected from eight new subjects (five samples per posture per subject) who did not contribute to the static posture database. The ranges of subject’s height and weight are 160–191 cm and 65.9–93.6 kg, respectively. These anthropometric values are within those represented in the static posture database. Shown in Fig. 8 (solid line in the right graph) are the classification accuracies averaged over postures as a function of number of eigenvectors used in classification. Compared with Fig. 7, it is clear that classification performance is better with subjects the system is “familiar with.” In an effort to locate the sources of error, we examined the posture labels associated with not only the minimum DFPS,  $\min \varepsilon$  (the first choice), but also those with the next two smallest  $\varepsilon$  values (the second and third choices). The results are shown as dashed lines in the right graph of Fig. 8 for new subjects. The middle and top curves (dashed and dotted lines, respectively) reveal the classification accuracies that can be potentially achieved if the correct posture label is associated with the first two or three smallest  $\varepsilon$  values, respectively. The corresponding results for the pressure maps collected from “familiar” subjects are shown on the left of Fig. 8. Note that the top curves in both graphs of Fig. 8 are in the upper nineties, indicating that similar performance levels with both “familiar” and new subject groups can be achieved if the correct posture label can be derived from the first three smallest  $\varepsilon$  values.

Execution time for the classification subroutine as a function of number of eigenvectors used has also been measured, with source codes that have yet to be optimized for speed. This is an important parameter for any real-time application of our system. The average classification time for 5, 10, 15, or 20 eigenvectors is 62.1, 107.8, 168.1, or 241.0 ms, respectively. The corresponding average classification accuracy (for “familiar” subjects) is 88, 95, 96, or 96%, respectively. In view of these measurements,  $M' = 15$  (out of  $M = 150$ ) eigenvectors corresponding to the 15 largest eigenvalues are used for the static posture classification system.

## VI. SUMMARY

We have described a static posture classification system based on a sensing chair that monitors the pressure distribution patterns on its surfaces in real time. The PCA technique, commonly used in computer and robot vision, has been successfully applied to the problem of posture classification from pressure maps. A PCA-based algorithm has the advantage of being very fast. Its disadvantage is the lack of physical interpretations associated with eigenposture spaces. Our current system runs in real-time (with an update rate of roughly 6 Hz) on a Pentium PC in Windows 98 environment. Average classification accuracy is 96% for subjects the system had felt before, and 79% for those who are new to the system. We are currently investigating ways to improve the system's accuracy for new subjects by taking into account the first three eigenposture spaces that are closest to the test pressure map. Future work is aimed toward a dynamic posture tracking system that continuously tracks not only steady-state (static) but transitional (dynamic) sitting postures.

## ACKNOWLEDGMENT

The authors wish to thank Dr. B. Moghaddam for the MATLAB code used in computing eigenposture spaces from training data. The comments from the three anonymous reviewers are greatly appreciated.

## REFERENCES

- [1] R. I. Barnett and F. E. Shelton, "Measurement of support surface efficacy: Pressure," *J. Prevent. Healing: Adv. Wound Care*, vol. 10, no. 7, pp. 21–29, 1997.
- [2] J. A. Birke, J. G. Foto, S. Deepak, and J. Watson, "Measurement of pressure walking in footwear used in leprosy," *Lepra Rev.*, vol. 65, pp. 262–271, 1994.
- [3] R. A. Brooks, "Model-based three-dimensional interpretations of two-dimensional images," *IEEE Trans. Pattern Anal. Machine Intell.*, vol. 5, pp. 140–150, 1983.
- [4] M. H. Coen, "The future of human-computer interaction, or how I learned to stop worrying and love my intelligent room," *IEEE Intell. Syst.*, vol. 14, pp. 8–10, Mar./Apr. 1999.
- [5] D. Cohen, "An objective measure of seat comfort," *J. Aviat., Space Environ. Med.*, vol. 69, pp. 410–414, 1998.
- [6] S. F. Conti, R. L. Martin, E. R. Chaytor, C. Hughes, and L. Luttrell, "Plantar pressure measurements during ambulation in weightbearing conventional short leg casts and total contact casts," *Foot Ankle Int.*, vol. 17, pp. 464–469, 1996.
- [7] P. Coy, "Ready for its maiden flight: A new airline seat," *Bus. Week*, pp. 199–199, Nov. 1996.
- [8] J. L. Flanagan, "Autodirective sound capture: Toward smarter conference rooms," *IEEE Intell. Syst.*, vol. 14, pp. 16–19, Mar./Apr. 1999.
- [9] D. Franklin, "The intelligent classroom," *IEEE Intell. Syst.*, vol. 14, pp. 2–5, Sept./Oct. 1999.
- [10] K. Fukunaga, *Introduction to Statistical Pattern Recognition*, 2nd ed. New York: Academic, 1990.
- [11] T. Harada, T. Mori, Y. Nishida, T. Yoshimi, and T. Sato, "Body parts positions and posture estimation system based on pressure distribution image," in *Proc. 1999 IEEE Int. Conf. Robotics and Automation*, Detroit, MI, May 1999, pp. 968–975.
- [12] E. C. Hughes, W. Shen, and A. Vertiz, "The effects of regional compliance and instantaneous stiffness on seat back comfort," in *SAE Tech. Paper Series*, 1998, no. 980 658, pp. 105–115.
- [13] R. Lueder and K. Noro, *Hard Facts About Soft Machines: The Ergonomics of Seating*. New York: Taylor & Francis, 1994.
- [14] G. A. Miller, "The magical number seven, plus or minus two: Some limits on our capacity for processing information," *The Psychol. Rev.*, vol. 63, pp. 81–97, 1956.
- [15] M. C. Mozer, "An intelligent environment must be adaptive," *IEEE Intell. Syst. Mag.*, vol. 14, pp. 11–13, Mar./Apr. 1999.
- [16] M. J. Mueller and M. J. Strube, "Generalizability of in-shoe peak pressure measures using the F-scan system," *Clin. Biomechan.*, vol. 11, pp. 159–164, 1996.
- [17] H. Murase and S. K. Nayar, "Visual learning and recognition of 3D objects from appearance," *Int. J. Comput. Vision*, vol. 14, pp. 5–24, 1995.
- [18] B. Noble and J. W. Daniel, *Applied Linear Algebra*. Englewood Cliffs, NJ: Prentice-Hall, 1988.
- [19] S. Oviatt, "Ten myths of multimodal interaction," *Commun. ACM*, vol. 42, pp. 74–81, 1999.
- [20] A. Pentland, "Perceptual intelligence," *Commun. ACM*, vol. 43, pp. 35–44, Mar. 2000.
- [21] A. Pentland, B. Moghaddam, and T. Starner, "View-based and modular eigenspaces for face recognition," in *Proc. IEEE Conf. Computer Vision and Pattern Recognition*, 1994, pp. 84–91.
- [22] P. Pentland, "Smart Rooms," *Scient. American*, vol. 274, pp. 68–76, Apr. 1996.
- [23] M. Reed and C. Grant, "Development of a measurement protocol and analysis techniques for assessment of body pressure distributions on office chairs," Univ. Michigan, Ann Arbor, 1993.
- [24] M. Roach, "Hot seat," *Discover*, pp. 74–77, Mar. 1998.
- [25] L. A. Slivovsky and H. Z. Tan, "A real-time sitting posture tracking system Purdue Univ. Tech. Rep.," Sch. Elect. Comput. Eng., Purdue Univ., West Lafayette, IN, TR-ECE 00-1.
- [26] H. Z. Tan, "A sensing chair," in *Proc. ASME Dynam. Syst. Contr. Div.*, vol. 67, New York, 1999, pp. 313–317.
- [27] H. Z. Tan, I. Lu, and A. Pentland, "The chair as a novel haptic user interface," in *In Proc. Workshop on Perceptual User Interfaces (PU'97)*, Banff, Alberta, Canada, Oct. 19–21, pp. 56–57, 1997.
- [28] H. Z. Tan and A. Pentland, "Tactual displays for wearable computing," *Personal Technol.*, vol. 1, pp. 225–230, 1997.
- [29] M. C. Torrance, "Advances in human-computer interaction: The intelligent room," in *Proc. CHI'95 Research Symp.*, Denver, CO.
- [30] *Proc. Workshop on Perceptual User Interfaces (PU'97)*, M. Turk, Ed., Banff, Alberta, Canada, Oct. 19–21, 1997.
- [31] *Proc. Workshop on Perceptual User Interfaces (PU'98)*, M. Turk, Ed., San Francisco, CA, Nov. 4–6, 1998.
- [32] M. Turk and A. Pentland, "Eigenfaces for recognition," *J. Cognitive Neurosci.*, vol. 3, pp. 71–86, 1991.



**Hong Z. Tan** (S'96–M'96) received the B.S. degree in biomedical engineering and computer science from Shanghai Jiao Tong University, P. R. China, in 1986, and the S.M. and Ph.D. degrees in electrical engineering and computer science from the Massachusetts Institute of Technology (M.I.T.), Cambridge, in 1988 and 1996, respectively.

She is an assistant professor with the School of Electrical and Computer Engineering, Purdue University, West Lafayette, IN. From 1996 to 1998, she was a research scientist at the M.I.T. Media Laboratory, where she initiated the sensing chair project. Her research interests include an information-based framework for interface design and evaluation, pattern recognition algorithms for distributed contact sensors, and psychophysical studies of haptic displays.



**Lynne A. Slivovsky** received the B.S. degree in computer and electrical engineering and the M.S. degree in electrical engineering from Purdue University, West Lafayette, IN, in 1992 and 1993, respectively. She is currently a doctoral student in the School of Electrical and Computer Engineering, Purdue University.

She has interned at Lexmark International, Sunnyvale, FL, Compaq Computer Corporation, Houston, TX, and CESAR Lab at Oak Ridge National Laboratory, Oak Ridge, TN, where she worked on vision-based tracking of mobile robots. Her research interests include machine vision, pattern recognition, human-computer interfaces, perceptual grouping, and gesture recognition.



**Alex (Sandy) Pentland** (M'00) is the academic head of the Massachusetts Institute of Technology Media Laboratory, Founder, and Director of the Center for Future Health, and of the LINCOS Foundation. His overall focus is on using digital technology for the worldwide reinvention of health, education, and community. Toward this end, he has done research in wearable computing, human-machine interface, computer graphics, artificial intelligence, machine and human vision, and has published more than 200 scientific articles in these areas.

Dr. Pentland has recently been named by *Newsweek* magazine as one of the 100 Americans most likely to shape the next century. He has won awards from several academic societies, including the American Association for Artificial Intelligence and *Ars Electronica*.